The effect of tunable modification parameters on the structure and properties of polypropylene with cyclotrimerization surface of isocyanates

Menghan Sun,[1] Xianming Zhang,[1] Wenxing Chen,[1] Lianfang Feng[2]

[1]Key Laboratory of Advanced Textile Materials and Manufacturing Technology, Ministry of Education, Zhejiang Sci-Tech University, Hangzhou 310018, China
[2]State Key Laboratory of Chemical Engineering, Department of Chemical and Biochemical Engineering, Zhejiang University, Hangzhou 310027, China
Correspondence to: X. M. Zhang (E-mail: joolizxm@hotmail.com)

ABSTRACT: The cyclotrimerization of methylene diphenyl 4,4-diisocyanate (MDI) and 3-isopropenyl-α,α'-dimethylbenzene isocyanate (TMI) was applied on the bead/membrane surfaces of a polypropylene (PP)-bearing isocyanate group to synthesize a protective networked polymer. Chemical structures of these molecules were characterized through attenuated total reflectance–Fourier transform infrared spectroscopy. Results showed that the absorption peak of isocyanate group at 2255 cm^{-1} became negligible after the reaction was completed. The absorption peaks of the isocyanurate groups appeared simultaneously at 1600 cm^{-1} and at 1510–1560 cm^{-1}; this result indicated that the grafted isocyanates were almost consumed, thereby forming isocyanurates. Energy X-ray dispersive spectroscopy revealed that oxygen content increased; indeed, isocyanurate was formed on the PP surface. Pure PP beads, PP-g-TMI, and cyclotrimerization products were also subjected to thermal property tests to investigate their corresponding thermal stabilities. Cyclotrimerization could result in the increase in PP-grafted decomposition temperature, even slightly higher than pure PP. Rheological behavior in oscillatory flow was also evaluated; the storage modulus, loss modulus, and complex viscosity of cyclotrimerization products were higher than those of the PP-grafted membranes. Surface morphology was further observed through field-emission scanning electron microscopy and atomic force microscopy. The cyclotrimerization products contained blocks and exhibited a rough surface. © 2015 Wiley Periodicals, Inc. J. Appl. Polym. Sci. **2016**, *133*, 43327.

INTRODUCTION

1,3,5-Triazinane-2,4,6-triones, known as isocyanurate, is a material with a stable six-cyclic structure without an active hydrogen atom; with these characteristics, the moieties possess specific rigidity, thermal resistance, and hydrolytic stability.[1–3] Therefore, isocyanurates formed through the cyclotrimerization of a wide range of isocyanates are used to modify polyurethanes and coating materials to obtain various properties, such as enhanced thermal and chemical resistance, flame retardation, and film-forming characteristics.[4–7]

However, studies on isocyanurate preparation have mainly focused on cyclotrimerization conditions, especially the selection of catalysts, such as phosphines,[8] various metal fluorides,[9] amines,[10] calcium carbene complexes,[11] pyrrolyl lithium complexes,[12] and N-heterocyclic carbenes[13,14]; as a consequence, isocyanurate is rapidly and quantitatively formed. Moghaddam et al.[15] reported that a combination of sodium p-toluenesulfinate (pTolSO$_2$Na) and tetrabutylammonium iodide efficiently catalyzes the cyclotrimerization of isocyanates. Moritsugu et al.[16–18] comprehensively investigated the selective and quantitative cyclotrimerization between MDI and aliphatic/aromatic isocyanates by using pTolSO$_2$Na as single catalyst and 1,3-dimethylimidazolidinone (DMI) as an aprotic polar solvent. The induced catalytic activity can be explained by the presence of the negative charge on oxygen atoms and the alpha effect from sulfur atom, which contains a pair of nonbonding electrons to attack isocyanates as hard heterophile, and the results indicate the aliphatic isocyanates are easier than the aromatic to take cyclotrimerization.[17]

Polypropylene (PP) is one of the most significant commercial polymers produced on an industrial scale because this substance is characterized by low-cost, excellent impact resistance, mechanical toughness, and resistance to chemical attack and aging.[19–21] However, the nonpolar nature of PP is a large disadvantage causing
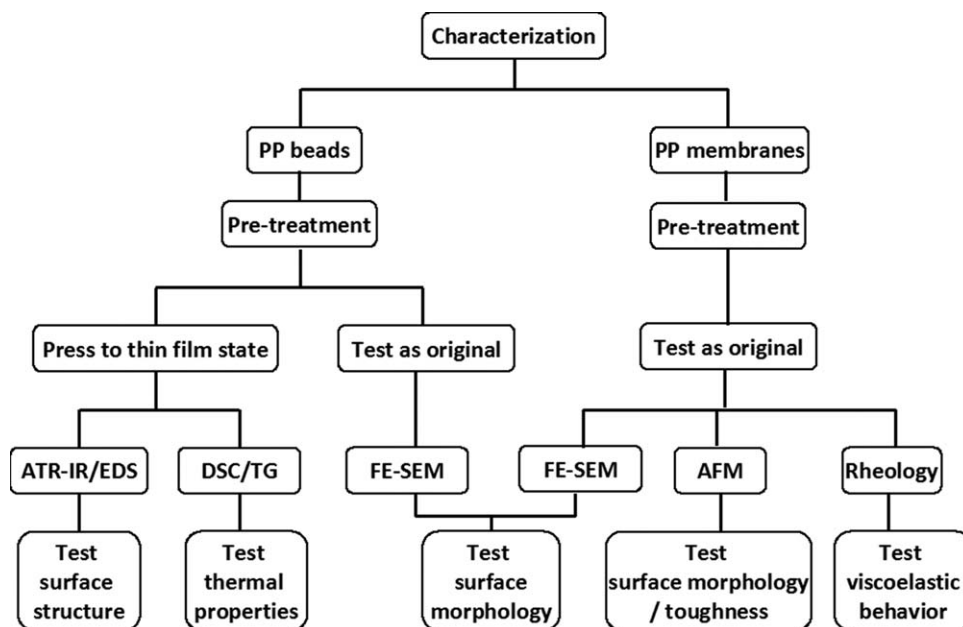
Figure 1. Flow chart of the characterization of different samples.

hydrophobia and poor interfacial adhesion onto other polar materials.[22] Although various modified polypropylene molecules have been extensively investigated,[23–27] these modifications often weaken the thermal and mechanical properties. In this study, an effective method was applied to modify PP to provide networked structures bearing isocyanurate moieties on the surface; these moieties were synthesized through the cyclotrimerization of isocyanates to form a polymer with a protective network. We intended to cover PP plastics with surface-networked polymer to study further improvement of PP thermal properties. So, PP samples can have more high-strong application without the loss of PP matrix itself, and this study can even be as a model of surface modification for other materials. PP-bearing isocyanate groups were functionalized in a solid state before cyclotrimerization was performed to modify the PP surface. The borane/O_2 system, which is a radical initiation system, can graft the vinyl monomer with functional groups.[26,28,29]

In this study, 3-isopropenyl-α,α'-dimethylbenzene isocyanate (TMI), which contains a reactive double bond and an isocyanate group (–NCO), was introduced as a grafted monomer to the PP surface. On the basis of the prepared PP-g-TMI with –NCO groups outside the particles,[29] we had briefly studied the thermal properties of the cyclotrimerized PP. Differently, here, we targeted the synthesis conditions of the networked polymer on the surface subjected to the cyclotrimerization between the grafted –NCO and MDI. Besides, we subsequently characterized the surface morphological and rheological properties by superficially modifying PP membranes.

EXPERIMENTAL

Materials
Commercial-grade PP beads were purchased from Nanjing Yangzi Petrochemicals (F401) (China); precursor membranes from the PP beads were prepared by hot compression molding with a fixed circular size (20 mm in diameter and approximately 0.6 mm in thickness) at 200°C. The beads and membranes were ultrasoni-cally washed with ethanol and dried under 60°C with reduced pressure before use. In this research, we characterized PP beads with ATR-IR, EDS, TG/DSC, and SEM to test its preliminary properties, like structural and thermal properties; and characterized the surface and rheological property on PP membranes through FE-SEM, AFM, and rotational rheometer. A solution of triethylborane (Et$_3$B) in tetrahydrofuran (THF, 1.0 M) was purchased from Chengdu Xiya Reagent Research Center (China) and used as received. The TMI monomer was purchased from J&K Scientific Ltd. The diisocyanate compound MDI (98%), catalyst pTolSO$_2$Na (98%), and solvent DMI (98%) were purchased from Aladdin Chemistry Co., Ltd. (USA) and used as received. Acetone was purchased from Zhejiang San-ying Chemical Reagent Co., Ltd. (China) and used as received.

Table I. Reaction Conditions and Thermal Properties of the Products Obtained through Cyclotrimerization Affected by the Catalyst[a]

Entry	Product	pTolSO$_2$Na (mol % to –NCO)	T_m (°C)	T_{d5} (°C)	T_{d10} (°C)
1	PP	—	165.9	412.3	425.7
2	PP-g-TMI	—	161.9	394.9	418.0
3	**A[b]1**	0.5	165.2	404.3	421.0
4	**A2**	1	165.8	405.0	421.0
5	**A3**	3	165.2	403.0	420.3
6	**A4**	5	164.9	407.0	423.0
7	**B[c]1**	0.5	—	397.7	417.7
8	**B2**	1	—	391.7	413.1
9	**B3**	3	—	393.0	413.7

[a] The conditions shown here were set as [TMI]$_0$/[MDI]$_0$ = 1:8, 80°C, and for 24 h.
[b] **A** shows the results after the products were washed.
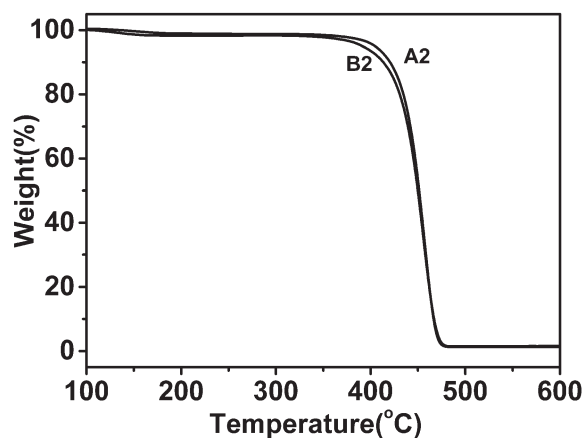[c] **B** shows the results of the products that were not washed with water.

Figure 2. TG curves of the products washed with water (**A2**) or not washed with water (**B2**).

Figure 4. DSC curves of (a) pure PP beads, (b) PP-g-TMI, and cyclotrimerization products of (c) **A4**, (d) **C1**, (e) **C2**, and (f) **C3** obtained at different coannulation levels.

Measurements

Attenuated total reflectance Fourier transform infrared spectroscopy (ATR-IR) spectra was recorded on a Nicolet 5700 spectrometer equipped with a composite of diamond/ZnSe crystal within the range of 650–4000 cm^{-1}, a resolution of 2 cm^{-1}, and a scanning frequency of 64 times. The tested bead samples were prepared by being pressed onto films before water-washing.

Differential scanning calorimetry (DSC) was performed on a Mettler Toledo DSC Analyzer under nitrogen flow. The test samples were prepared after the beads were pressed into film states and cut into the pieces with the needed mass of 4 mg. The samples were initially heated at the speed of 20°C/min from 25 to 200°C, held at 200°C for 3 min to erase the residual thermal history, and then cooled at the rate of 50°C/min to 25°C. The second heating performed at a heating rate of 25°C/min. The melting temperature (T_m) was obtained from the curve.

Thermal gravimetric analysis (TGA) was performed using a Mettler Toledo thermogravimetric analyzer. The test samples were prepared after the beads were pressed into film states and cut into the pieces with the needed mass of 8 mg. And the test
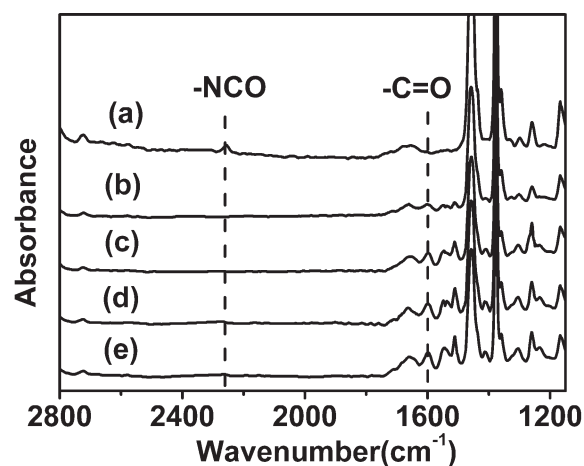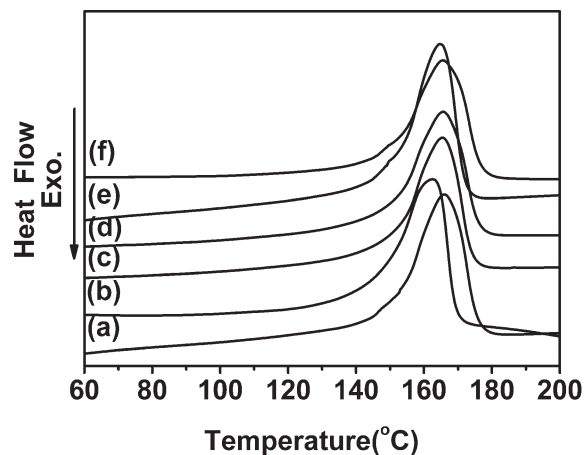
procedure was set as heating at a range of 25 to 600°C with a rate of 20°C/min in nitrogen flow. Decomposition temperature (T_d) was obtained from the curve. The corresponding experiment results have general trend with different variables, so here we took only one set of experiment results into tables.

The surface morphological characteristics of the PP beads and the PP membranes were examined through ULTRATM 55 field-emission scanning electron microscopy (FE-SEM) at 1 kV acceleration voltage. The samples were sputtered with gold before measurement was performed because the polymer exhibited poor electrical conductivity. An *in situ* surface elemental analysis via EDS was performed under an accelerating voltage of 5 kV. Gold was then eliminated.

The rheological behavior of the PP membranes in oscillatory flow was characterized by using an Anton Paar rotational rheometer (Physica MCR 301) and CTD 450 convection oven (Anton Paar). The samples were melted at the prescribed temperature of 200°C for 5 min to remove the residual thermal history before the experiments were performed.

Tapping mode atomic force microscopy (TM-AFM) was performed by using a PSIA XE-100E system. The AFM topography

Figure 3. ATR-IR spectrum of (a) PP-g-TMI and the cyclotrimerization products of (b) **A4**, (c) **C1**, (d) **C2**, and (e) **C3**.

Table II. Reaction Conditions and Thermal Properties of the Cyclotrimerization Products Obtained through the Coannulation of the TMI-Grafted Material and MDI[a]

Entry	Product	$[TMI]_O/[MDI]_O$ (mol ratio)	T_m (°C)	T_{d5} (°C)	T_{d10} (°C)
1	PP	—	165.9	412.3	425.7
2	PP-g-TMI	—	161.9	394.9	418.0
3	**A4**	1:8	164.9	407.0	423.0
4	**C1**	1:10	165.2	405.7	423.0
5	**C2**	1:20	164.9	411.0	425.7
6	**C3**	1:30	165.3	415.7	425.7

[a] The conditions shown here were set at $pTolSO_2Na$(mol %) = 5% (—NCO), at 80°C for 24 h. All the products were washed with water.
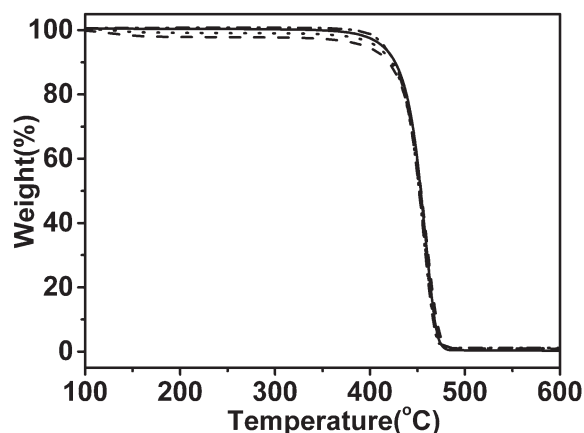
Figure 5. TG curves of pure PP beads (solid line), PP-g-TMI (dashed line), and cyclotrimerization products of **A4** (dotted line) and **C3** (dotted–dashed line).

images of the PP membranes with a scan range of 10 μm3 were obtained in the air under ambient conditions.

Figure 1 briefly explained the characterization and intention for different samples with corresponding pretreatment. In this article, we characterized the structural and thermal properties on PP beads with ATR-IR, EDS, and TG/DSC, SEM; and characterized the surface morphology and rheology properties on PP membranes through FE-SEM, AFM, and rotational rheometer. The reason why the characterizations were such classified is that the membranes are fit to test the viscoelastic behavior of samples. Meanwhile, in order to apparently certify the existence of cyclotrimerization products, we took advantage of some other characterization tests, involving the surface roughness from AFM associating with the surface morphology in the flat state from SEM.

Free-Radical Graft Polymerization of TMI onto the Surface of the PP Beads
The grafting reactions were mainly performed in a three-necked flask where the rotor was gently rotating. Three-hundred milligrams PP beads (about 4 mm in diameter, 15 pieces) were placed in the three-necked flask and protected under nitrogen atmosphere. A solution of Et$_3$B in THF (1.0 M:3.0 mL, 3.0 mmol) was added and stirred slowly under nitrogen atmosphere and removed by using a pipette after 12 h. All of the PP semi-finished products were placed in a vacuum drying oven for quick drying. TMI (3 mL, 15.2 mmol) was added to the treated PP by connecting to the beads under nitrogen atmosphere. A mass of

air was then bubbled into the flask at the liquid level. After 6 h, the resulting products were removed, sonicated, flushed with acetone four times, and dried in a vacuum at 60°C. Grafting reaction on the PP membranes was similar to that of the PP beads. The mechanism of grafted material synthesis is described in a previous study.[29]

Cyclotrimerization of MDI with PP-g-TMI
The grafted PP with a graft ratio of approximately 3.0% was kept under a nitrogen atmosphere in the three-necked flask. Quantitative pTolSO$_2$Na (mol % to −NCO groups) was added, and a well-mixed solution of MDI in DMI was infused into the flask. After the solution was stirred at 80°C for a prescribed time, the residue was removed; the solid particles/membranes were ultrasonically washed and flushed four times with acetone. The obtained PP beads were vacuum dried at 60°C at reduced pressure for 24 h. The cyclotrimerization of MDI with the grafted TMI is also described in a previous study.[29]

RESULTS AND DISCUSSION

Cyclotrimerization of MDI with the Grafted TMI at PP Beads Surface
Before isocyanates were subjected to cyclotrimerization, the parameters of grafting TMI onto PP and those that could control the graft ratio at a constant value of 3.0% under certain conditions were investigated.[29] Based on having conducted simple cyclotrimerization on the surface of PP beads, this study focused on the effects of catalyst dosage, watering products or not, initial mixture ratios ([TMI]$_0$/[MDI]$_0$), and reaction time.

The effect of the catalyst on melting temperature and decomposition temperature was investigated (Table I). Cyclotrimerization occurred on the bead surface; after ATR-IR tests were performed, the products were immersed in water to remove the water-soluble pTolSO$_2$Na. The products washed with water yielded higher decomposition temperatures at 5% and 10% weight loss, (T_{d5} and T_{d10}, respectively) compared with those that were not washed with water. The TG curves of the products washed and not washed with water were also compared (Figure 2). The TG curves of the products washed with water exhibited higher decomposition temperature and weight loss because the residual catalyst promotes the thermal decomposition of the networked polymer.[18] However, the effect of the catalyst was not evident; this finding is similar to that described in other studies, which consider catalyst doses as the only variable. This phenomenon is due to the heterogeneous reaction system, in contrast to a two-component well-mixed homogeneous system.[16] The catalyst was

Table III. Different TG Test Results of Cyclotrimerization Products Obtained at the Same Coannulation of the TMI-Grafted Material and MDI

[TMI]$_0$/[MDI]$_0$ (mol ratio)	T_{d5} (°C)	T_{d10} (°C)	T_{d5} (°C)	T_{d10} (°C)	T_{d5} (°C)	T_{d10} (°C)
	Test 1		Test 2		Test 3	
1:8	407.0	423.0	407.8	423.5	408.7	423.0
1:10	405.7	423.0	408.7	423.9	408.3	423.5
1:20	411.0	425.7	411.6	424.3	411.1	424.8
1:30	415.7	425.7	413.9	425.9	414.8	425.6
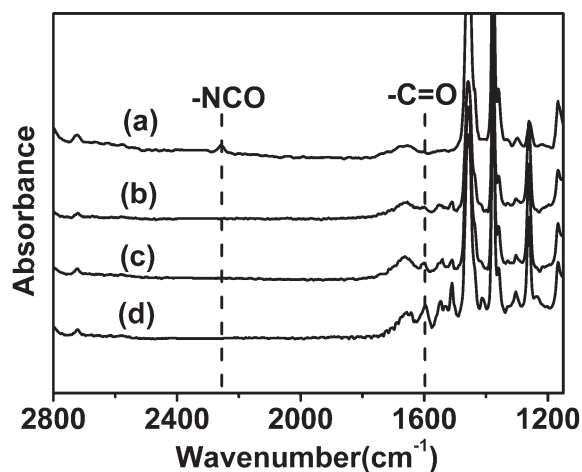
Figure 6. ATR-IR spectrum of (a) PP-g-TMI and cyclotrimerization products of (b) **D1**, (c) **D2**, and (d) **C1**.

Figure 8. TG curves of the cyclotrimerization products of **D1** (solid line), **D2** (dashed line), and **C1** (dotted line).

not applied completely to the cyclotrimerization of TMI-grafted material and MDI, some may induced the self-cyclotrimerization of MDI in the solution; thus, the catalyst dosage did not significantly affect T_{d5} and T_{d10} of modified PP materials.

In Figure 3, the absorption peak of the isocyanate groups at 2255 cm^{-1} became negligible after the cyclotrimerization of TMI and MDI was completed. This result indicated that the isocyanates were almost consumed. The absorption peak that appeared at approximately 1600 cm^{-1} was attributed to the carbonyl (—C=O) stretching vibration in the six-membered-ring structure. The absorption peaks at 1510–1560 cm^{-1} corresponded to the characteristic absorption peaks of isocyanurates. In these cases, the IR spectra confirmed that the isocyanates were completely consumed and the networked isocyanurate was successfully formed. The strength of the isocyanurate peaks was stronger than that of the isocyanate peaks because the contents of the formed isocyanurates were higher than those of the initially grafted —NCO. The networked structure was formed and the strength of carbonyl absorption was increased when the coannulation levels were low and the
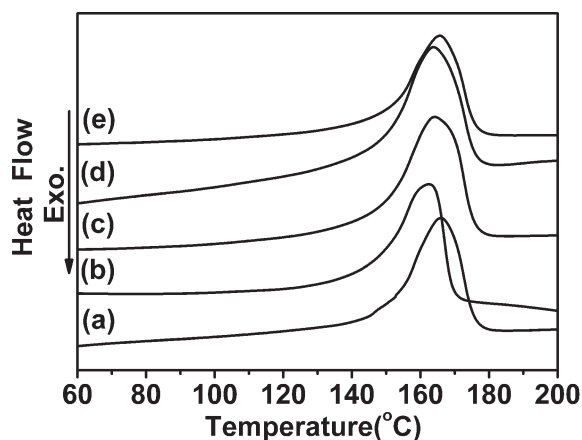
diisocyanate concentration was increased. The solution viscosity increased at high concentrations during heating. This process improved the self-cyclotrimerization of MDI in the solution; the cyclotrimerization on the surface of the beads remained at equilibrium; thus, the absorption peaks did not considerably change.

Based on the DSC spectrum in Figure 4 and the specific data in Table II, the melting temperature of PP-g-TMI (161.9°C) decreased compared with that of pure PP beads (165.9°C); by contrast, T_m returned to the melting temperature of the pure PP within the error range after cyclotrimerization was completed. Likewise, the TG spectrum in Figure 5 and the data in Table II showed that T_{d5} and T_{d10} of PP-g-TMI decreased significantly compared with the pure PP beads; after cyclotrimerization was completed, the decomposition temperatures likely increased. In the first stage, T_m and T_d decreased because the regular structure of the PP chains was disrupted; the PP chains were disrupted because the grafted TMI is a short chain forming a randomly branched structure.[30] The networked structure consisted of heterocyclic rings formed through cyclotrimerization. These rings were rigid structures limiting the motion of chains. Thus, the weakening of the thermal properties was caused by the grafting of short branches. In addition, MDI content also increased and the reticulated cross-link density

Figure 7. DSC curves of (a) pure PP beads, (b) PP-g-TMI, and cyclotrimerization products of (c) **D1**, (d) **D2**, and (e) **C1** obtained in different reaction times.
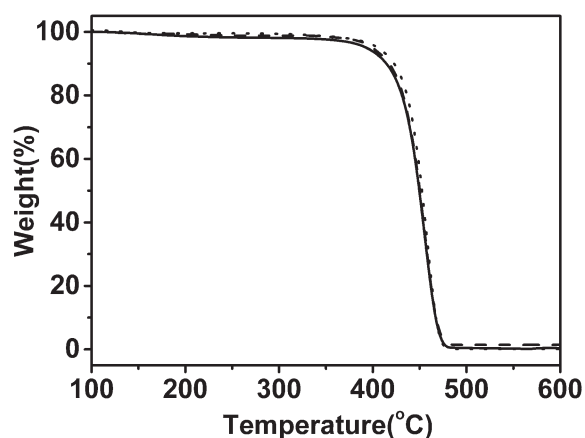
Table IV. Reaction Conditions and Thermal Properties of Cyclotrimerization Products Obtained at Different Reaction Times[a]

Entry	Product	Reaction time (h)	T_m (°C)	T_{d5} (°C)	T_{d10} (°C)
1	PP	—	165.9	412.3	425.7
2	PP-g-TMI	—	161.9	394.9	418.0
3	**D1**	8	164.0	393.7	415.0
4	**D2**	16	163.2	402.3	421.2
5	**C1**	24	165.2	405.7	423.0

[a] The conditions shown here were set at [TMI]$_0$/[MDI]$_0$ = 1:10, pTolSO$_2$Na (mol %) = 5% (—NCO), 80°C. All the products were washed with water.
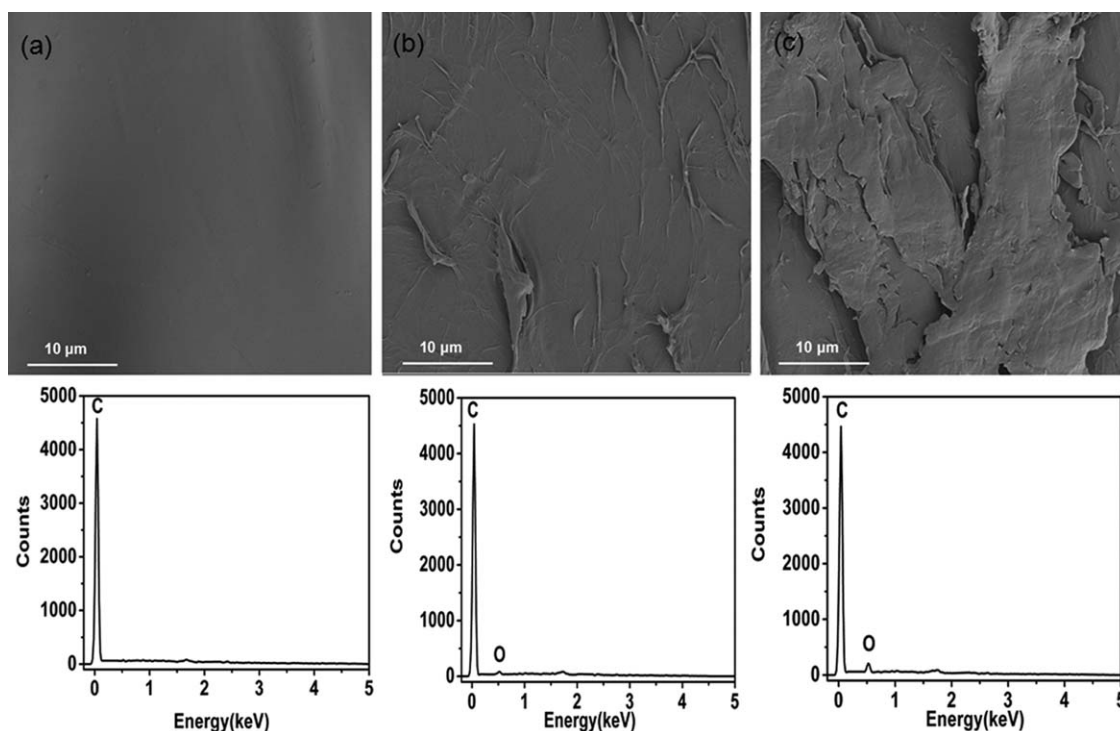
Figure 9. FE-SEM and EDS spectra of (a) pure PP bead, (b) PP-g-TMI, and (c) cyclotrimerization product of **C3**.

improved as $[TMI]_0/[MDI]_0$ increased. At high concentrations, the decomposition temperature of the grafted material could be equal to that of the pure PP beads; the TG curve of **C3** was higher than that of pure PP. This finding indicated that the reticulated cross-linking polymer covering the surface of PP slightly improved the heat resistance of the polymer. To ensure the reliability of TG data, the corresponding experiments were carried out for three times and tested at the same conditions, respectively. Now, the results have been listed in Table III, from which we can observe the results tested in the same condition have some distinction but not quite obvious, and the general changing trend stayed consistence. Taking this as an example, the next tables about thermal properties were listed by introducing just one experiment result which can represent the general trend accompanying the relative reaction conditions.

Figure 6 shows that the characteristic absorption peaks of isocyanates were notable, as indicated in the ATR-IR curves of the cyclotrimerization products obtained at <24 h reaction time, although the isocyanate groups were depleted. The aliphatic isocyanates were intrinsically less electrophilic, and the ability of these molecules to accept the nucleophilic attack of the sulfinate catalyst is limited.[31] PP-g-TMI requires more time to induce the cyclotrimerization of PP-g-TMI. Therefore, the degree of cyclotrimerization was lower in a short reaction time, resulting in a small variation in melting and decomposition temperatures. Compared with the temperatures of PP-g-TMI, the characteristic temperatures of cyclotrimerization-modified PP were significantly increased. The DSC curve in Figure 7, TG curve in Figure 8, and characteristic temperatures in Table IV showed that the heat resistance improved with longer reaction time because many cross-linking polymers covered the PP surface.

The surface chemical compositions were also characterized through EDS (Figure 9). After the grafting treatment was administered, oxygen element appeared as carbon content decreased; by contrast, oxygen content increased significantly after cyclotrimerization was completed. This result indicated that cyclotrimerization occurred on the PP surface. The morphological characteristics of the PP beads before and after modification are also shown in Figure 9; the result revealed that cyclotrimerization treatment caused a more distinct rough surface. These findings are consistent with those obtained through ATR-IR.

Cyclotrimerization of MDI with TMI Grafted on PP-Pieces Surface and Its Additional Properties

The ATR-IR characteristics and thermal properties of the PP beads were described. Additional properties after the surface of the PP membranes was modified were further investigated.

In Figure 10, the microscopic surfaces of the pure PP and the cyclotrimerization products on the membranes were scanned through FE-SEM. Scratches on the surface generated during the hot-pressed process were detected. With further reaction, large irregular blocks appeared on the PP membrane surface; this result indicated that cyclotrimerization was successful. However, the regions were relatively concentrated and scattered unevenly. The 3D approach to the surface of the pure PP membrane and the cyclotrimerized region was developed through AFM at 10 μm^2. This range provides a fair visual comparison of the conditions and products before and after cyclotrimerization occurred. In the scale, the brighter places represent the higher regions. Overall, the pure PP surface seemed smooth to some extent. The protuberance produced after cyclotrimerization occurred
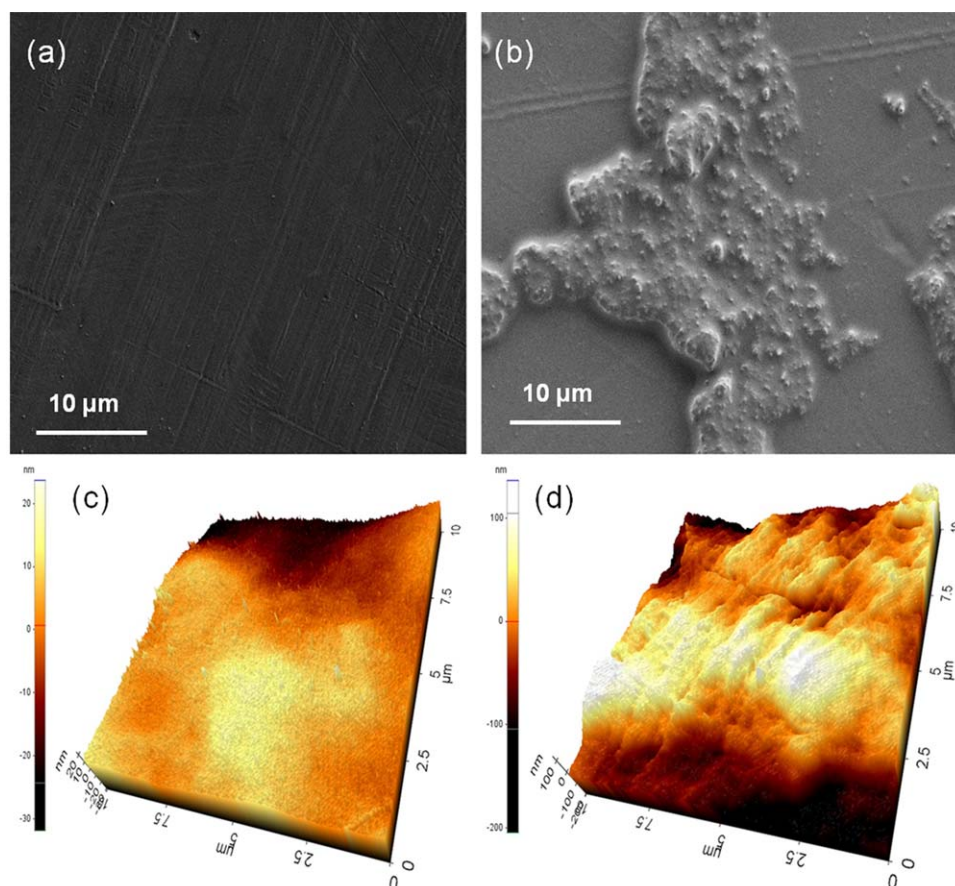
Figure 10. Surface topography of PP membranes at the same magnification of FE-SEM: (a) PP, (b) PP modified through cyclotrimerization. A three-dimensional approach to membrane surface modification in AFM: (c) PP and (d) PP modified through cyclotrimerization. [Color figure can be viewed in the online issue, which is available at wileyonlinelibrary.com.]

was also evident; in particular, height and roughness were improved (Table V).

The frequency sweep tests illustrated the linear viscoelastic behavior of the polymer. The tests were repeated at least twice by using fresh samples. We set 5 min as the resting period after the sample was loaded at the prescribed temperature of 200°C to remove the residual thermal history. The storage modulus G' and the loss modulus G'' increased as the angle frequency increased; the former represents elasticity and the latter denotes viscosity.[32] At the highest probed frequencies, the polymer matrix contribution dominated; at the lowest frequencies, the identity of the polymer composites becomes evident.[33]

Figure 11(a,b) shows the viscoelastic curves of the pure PP membrane, the PP-g-TMI, and the cyclotrimerized polymer with different coannulations. Elasticity and viscosity increased at low frequencies when cyclotrimerization coannulation increased; by contrast, both properties were similar at high frequencies. Figure 11(c) shows the frequency dependence of the complex viscosity of the modified PP. Compared with the complex viscosity of pure PP, the complex viscosity of the modified membranes decreased when molecular weight decreased. This finding may also be possible because the side-chains improved the spacing of

backbones; thus, interaction that may cause a decrease in viscosity is reduced. The viscosity of cyclotrimerized polymer was also higher than that of PP-g-TMI; this increase in viscosity was more apparent when MDI took a higher proportion. The slightly increased complex viscosity was proportional to the cross-linking network formed on the surface; by contrast, surface polarity was improved and molecular interaction increased. However, the cyclotrimerization modification on the surface did not remedy the decrease in molecular weight. Regardless of frequency level, the viscosity of cyclotrimerized polymer still remained lower than that of the pure PP. Therefore, cyclotrimerization slightly improved viscosity.

Table V. Roughness Values of the PP Membrane and the Modified Products[a]

Sample	PP	PP cyclotrimerization
Roughness (Ra)[b] (nm)	7.6	15.0

[a] The values correspond to Figure 10(c,d).
[b] Ra is the roughness of the arithmetic mean determined at the scanned area (10 μm^2).
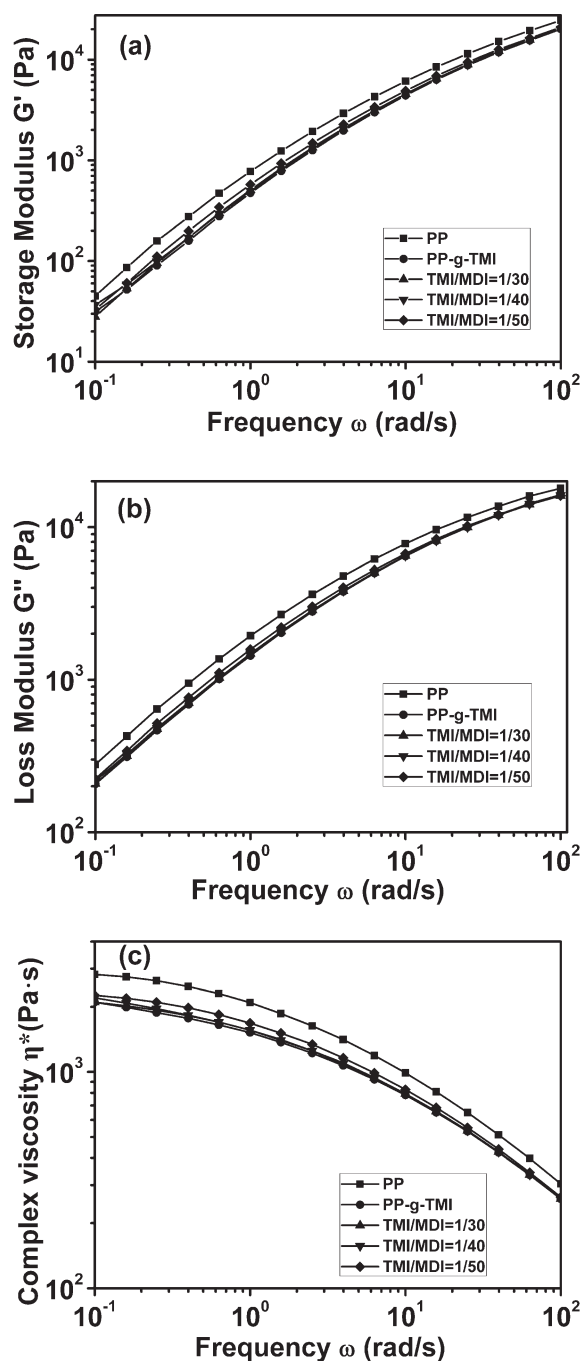
Figure 11. (a) Storage modulus G', (b) loss modulus G'', and (c) complex viscosity η^* as a function of the frequency of the products with different values of $[TMI]_0/[MDI]_0$.

CONCLUSIONS

In this study, cyclotrimerization was applied to form an isocyanurate-networked polymer on the PP bead/membrane surfaces. In addition, the reaction conditions of cyclotrimerization and the properties of cyclotrimerized products were investigated. The disappearance of the absorption peak of —NCO at 2255 cm^{-1} and the appearance of the absorption peak of isocyanurate at 1600 cm^{-1} and at $1510–1560 \text{ cm}^{-1}$ indicated that cyclotrimerization occurred on the PP surface. These results

were consistent with those obtained through EDS tests; oxygen content increased after cyclotrimerization was completed. The thermal properties were also characterized. The results demonstrated that the materials must be washed with water to remove residual $p\text{TolSO}_2\text{Na}$ and to improve the heat resistance of the products. After the PP surface was covered, the cyclotrimerized networked polymer compensated for the decrease in T_m and T_d of PP-g-TMI, with some even higher than pure PP. Moreover, the microstructure detected through FE-SEM and AFM revealed that many blocks were generated on the surface, and the roughness of the PP membrane surface was enhanced. We also investigated the rheological behavior in the oscillatory flow of the pure PP membrane, PP-g-TMI, and products under different cyclotrimerization conditions. The storage modulus, loss modulus, and complex viscosity of the PP membranes with cyclotrimerization were lower than those of pure PP membrane because of the limitation of modification structure and molecular mass. However, these properties were slightly improved compared with those of PP-g-TMI because of the formed networked structure. In all, due to some comprehensive reasons, such as the limited active groups and steric hindrance effect in cyclotrimerization process, the networked polymer did not reach the original expectation to cover all the PP surfaces to further improve the stability, but it did have some effect on the making up of PP-g-TMIs declination in the decomposition temperature.

REFERENCES

1. Herrmann, W. A.; Weskamp, T.; Bohm, V. P. W. *Adv. Organomet. Chem.* **2001**, *48*, 1.

2. Kordomenos, P. I.; Kresta, J. E. *Macromolecules* **1981**, *14*, 1434.

3. Wang, C. L.; Klempner, D.; Frisch, K. C. *J. Appl. Polym. Sci.* **1985**, *30*, 4337.

4. Lin, I. S.; Kresta, J. E.; Frisch, K. C. Reaction Injection Molding and Fast Polymerization Reactions; Plenum Publishing: New York, **1982**, p 147.

5. Tanaka, K.; Toda, F. *Chem. Rev.* **2000**, *100*, 1025.

6. Sugimoto, H.; Yamane, Y.; Inoue, S. *Tetrahedron: Asymmetry* **2000**, *11*, 2067.

7. Peters, S. J.; Klen, J. R.; Smart, N. C. *Org. Lett.* **2008**, *10*, 4521.

8. Tang, J. S.; Mohan, T.; Verkade, J. G. *J. Org. Chem.* **1994**, *59*, 4931.

9. Nambu, Y.; Endo, T. *J. Org. Chem.* **1993**, *58*, 1932.

10. Moghaddam, F. M.; Dekamin, M. G.; Koozehgari, G. R. *Lett. Org. Chem.* **2005**, *22*, 734.

11. Orzechowski, L.; Harder, S. *Organometallics* **2007**, *26*, 5501.

12. Guo, Z. Q.; Wang, S.; Tong, H. B.; Chao, J. B.; Wei, X. H. *Inorg. Chem. Commun.* **2013**, *33*, 68.

13. Duong, H. A.; Cross, M. J.; Louie, J. *Org. Lett.* **2004**, *66*, 4679.

14. Giuglio-Tonolo, A. G.; Spitz, C.; Terme, T.; Vanelle, P. *Tetrahedron Lett.* **2014**, *55*, 2700.

15. Moghaddam, F. M.; Dekamin, M. G.; Khajavi, M. S.; Jalili, S. *Bull. Chem. Soc. Jpn.* **2002**, *75*, 851.

16. Moritsugu, M.; Sudo, A.; Endo, T. *J. Polym. Sci. Part A: Polym. Chem.* **2011**, *49*, 5186.

17. Moritsugu, M.; Sudo, A.; Endo, T. *J. Polym. Sci. Part A: Polym. Chem.* **2012**, *50*, 4365.

18. Moritsugu, M.; Sudo, A.; Endo, T. *J. Polym. Sci. Part A: Polym. Chem.* **2013**, *51*, 2631.

19. He, Q.; Yuan, T.; Wei, S.; Guo, Z. *J. Mater. Chem. A* **2013**, *11*, 13064.

20. Zhu, S.; Chen, J.; Li, H.; Cao, Y.; Yang, Y.; Feng, Z. *Appl. Clay Sci.* **2014**, *87*, 303.

21. Diop, M. F.; Torkelson, J. M. *Polymer* **2013**, *54*, 4143.

22. Rätzsch, M.; Arnold, M.; Borsig, E.; Bucka, H.; Reichelt, N. *Prog. Polym. Sci.* **2002**, *27*, 1195.

23. Gupta, B.; Saxena, S.; Ray, A. *J. Appl. Polym. Sci.* **2008**, *107*, 324.

24. Kim, H. J.; Lee, K. J.; Seo, Y. *Macromolecules* **2002**, *35*, 1267.

25. Li, J. L.; Xie, X. M. *Polymer* **2012**, *53*, 2197.

26. Okamura, H.; Sudo, A.; Endo, T. *J. Polym. Sci. Part A: Polym. Chem.* **2009**, *47*, 6163.

27. Thakur, V. K.; Vennerberg, D.; Kessler, M. R. *Appl. Mater. Interfaces* **2014**, *66*, 9349.

28. Wang, Z. M.; Hong, H.; Chung, T. C. *Macromolecules* **2005**, *38*, 8966.

29. Sun, M. H.; Zhang, X. M.; Chen, W. X.; Feng, L. F. *J. Appl. Polym. Sci.* **2015**, *132*, 42186.

30. Mousavi-Saghandikolaei, S. A.; Frounchi, M.; Dadbin, S.; Augier, S.; Passaglia, E.; Ciardelli, F. *J. Appl. Polym. Sci.* **2007**, *104*, 950.

31. Caraculacu, A. A.; Coseri, S. *Prog. Polym. Sci.* **2001**, *26*, 799.

32. Li, J.; Yi, L.; Lin, H.; Hou, R. *J. Polym. Sci. Part A: Polym. Chem.* **2011**, *49*, 1483.

33. Vermant, J.; Ceccia, S.; Dolgovskij, M. K.; Maffettone, P. L.; Macosko, C. W. *J. Rheol.* **2007**, *51*, 429.